JOURNAL OF GUIDANCE, CONTROL, AND DYNAMICS
Vol. 39, No. 1, January 2016

Quaternion Variational Integrators for Spacecraft Dynamics

Zachary R. Manchester* and Mason A. Peck†
Cornell University, Ithaca, New York 14850

DOI: 10.2514/1.G001176

A general method for deriving variational integrators for systems with quaternion state variables is introduced. These integrators exhibit realistic energy and momentum behavior while having computational costs comparable to or less than low-order Runge–Kutta methods, making them suitable for both simulation and real-time estimation and control applications. Integrators are derived for several systems, including rigid bodies with momentum actuators and internal viscous damping. Numerical examples illustrate the performance of the integrators and an application to attitude determination using an extended Kalman filter is presented.

Nomenclature

C	=	damping constant, kg · m^2 · s^{-1}
F	=	quaternion generalized force, kg · m^2 · s^{-2}
$\boldsymbol{F}_d$	=	discrete generalized force, kg · m^2 · s^{-1}
f, q	=	unit quaternions
h	=	time step, s
I	=	inertia matrix in body-fixed axes, kg · m^2
J	=	augmented inertia matrix in body-fixed axes, kg · m^2
k	=	time index
L	=	Lagrangian, kg · m^2 · s^{-2}
L_d	=	discrete Lagrangian, kg · m^2 · s^{-1}
m	=	rotor mass, kg
p	=	angular momentum in body-fixed axes, kg · m^2 · s^{-1}
S	=	action, kg · m^2 · s^{-1}
S_d	=	discrete action, kg · m^2 · s^{-1}
t	=	time, s
$\boldsymbol{x}$	=	rotor position in body-fixed axes, m
$\boldsymbol{\gamma}, \boldsymbol{\phi}$	=	three-parameter incremental rotations
δ	=	variational derivative
ϵ	=	small scalar
$\boldsymbol{\eta}$	=	arbitrary perturbation
$\boldsymbol{\rho}$	=	rotor angular momentum in body-fixed axes, kg · m^2 · s^{-1}
$\boldsymbol{\tau}$	=	external torque in body-fixed axes, kg · m^2 · s^{-2}
$\boldsymbol{\omega}$	=	angular velocity in body-fixed axes, rad · s^{-1}

I. Introduction

VARIATIONAL integrators have many advantages over Runge–Kutta methods and other traditional algorithms for numerically integrating equations of motion for mechanical systems. Rather than deriving differential equations of motion for a given system in continuous time, then discretizing them, variational approaches begin by discretizing the Lagrangian and the action integral for the system. The tools of variational mechanics are then used to derive discrete-time equations of motion. Integrators derived in this way retain many of the properties of the continuous system, such as momentum and energy conservation [1]. These integrators are also computationally efficient and stable, even for relatively large fixed time steps, making them well suited for use in real-time estimation and control applications.

Received 24 November 2014; revision received 22 February 2015; accepted for publication 28 February 2015; published online 10 April 2015.

*Graduate Student, Sibley School of Mechanical and Aerospace Engineering, 127 Upson Hall. Student Member AIAA.

†Associate Professor, Sibley School of Mechanical and Aerospace Engineering, 208 Upson Hall. Member AIAA.

Examples of integration methods that respect motion integrals of mechanical systems, often called geometric or symplectic integrators, have been known for decades. The classic example is the Verlet or Störmer–Verlet method [2,3]. These early methods were often devised in ad hoc ways that do not generalize well to arbitrary mechanical systems or higher orders of accuracy. More recently, systematic methods for deriving symplectic integrators using discrete-time versions of ideas from variational mechanics have been introduced [1]. These methods are straightforward applications of Lagrangian and Hamiltonian dynamics, and they can generate integration schemes of any desired order of accuracy.

Discrete variational mechanics has previously been applied to problems in rigid-body dynamics and the optimal control of rigid bodies using rotation matrices to parameterize attitude [4–6]. Momentum-preserving integrators have also been derived by other (nonvariational) means for rigid-body dynamics using quaternions to parameterize attitude [7–11]. The primary contribution of this paper is the application of discrete variational mechanics to spacecraft attitude dynamics using quaternion state variables. The emphasis on quaternions over other attitude parameterizations here is due to both the compact and elegant derivations they enable and their prevalence in the implementation of spacecraft guidance, navigation, and control algorithms. Specifically, they lend themselves to straightforward feedback control and estimation schemes of practical relevance in flight software.

The paper proceeds as follows. Section II gives a brief review of quaternions and outlines the notation used throughout the paper. Section III derives the classical Euler equation of rigid-body dynamics in continuous time using Hamilton's principle. Next, Sec. IV presents this derivation in discrete time, leading to the variational integrator presented in Sec. V. Sections VI–VIII incorporate several extensions to the basic rigid-body integrator, including reaction wheels, external torques, and internal damping. Finally, in Sec. IX, several numerical examples are presented, including an extended Kalman filter for attitude determination.

II. Background

Attitude dynamics and rotations are parameterized with quaternions throughout this paper. A brief review of their properties is presented in this section. A more thorough treatment is given by Altmann [12].

Quaternions form an algebra with a noncommutative binary product operation. It is often convenient to think of them as four-dimensional objects composed of a three-dimensional vector part $\boldsymbol{v}$ and a scalar part s:

$$q = \begin{bmatrix} \boldsymbol{v} \\ s \end{bmatrix} \tag{1}$$

This representation allows the quaternion product to be written in terms of scalar and vector products:

$$q_1 q_2 = \begin{bmatrix} \boldsymbol{v}_1 \times \boldsymbol{v}_2 + s_1 \boldsymbol{v}_2 + s_2 \boldsymbol{v}_1 \\ s_1 s_2 - \boldsymbol{v}_1 \cdot \boldsymbol{v}_2 \end{bmatrix} \tag{2}$$

Note that $q_1 q_2 \neq q_2 q_1$. Throughout the paper, quaternion products are indicated by juxtaposition, whereas scalar and vector products are indicated in the usual way, with the $\cdot$ and $\times$ symbols, respectively.

Rotations can be conveniently represented by unit-length quaternions. If $\boldsymbol{r}$ is a unit vector in $\mathbb{R}^3$ representing the axis of rotation and θ is the angle of rotation, then the quaternion representing the rotation is as follows:

$$q = \begin{bmatrix} \boldsymbol{r} \sin(\theta/2) \\ \cos(\theta/2) \end{bmatrix} \tag{3}$$

Both q and $-q$ correspond to the same rotation, making the unit quaternions a "double cover" of the group of rotations.

The conjugate of a quaternion is denoted with a superscript † and represents the rotation about the same axis $\boldsymbol{r}$ by $-\theta$:

$$q^\dagger = \begin{bmatrix} -\boldsymbol{v} \\ s \end{bmatrix} \tag{4}$$

Two rotations can be composed by multiplying their quaternion representations. A quaternion q_3 representing a rotation q_1 followed by a rotation q_2 is simply $q_3 = q_2 q_1$. The rotation of a three-dimensional vector $\boldsymbol{x}$ by a unit quaternion q is

$$\hat{\boldsymbol{x}}' = q \hat{\boldsymbol{x}} q^\dagger \tag{5}$$

where $\hat{\boldsymbol{x}}$ indicates the formation of a quaternion with zero scalar part from the vector $\boldsymbol{x}$:

$$\hat{\boldsymbol{x}} = \begin{bmatrix} \boldsymbol{x} \\ 0 \end{bmatrix} \tag{6}$$

Analytic functions can be defined for quaternion arguments in much the same way as for complex numbers and matrices. In particular, the quaternion exponential has a simple closed-form expression in terms of the quaternion's scalar and vector parts:

$$e^q = \sum_{n=0}^{\infty} \frac{q^n}{n!} = e^s \begin{bmatrix} \frac{\boldsymbol{v}}{|\boldsymbol{v}|} \sin(|\boldsymbol{v}|) \\ \cos(|\boldsymbol{v}|) \end{bmatrix} \tag{7}$$

The formula for a rotation quaternion in Eq. (3) can be compactly written in terms of the exponential:

$$e^{\hat{r}\theta/2} = \begin{bmatrix} \boldsymbol{r} \sin(\theta/2) \\ \cos(\theta/2) \end{bmatrix} \tag{8}$$

Finally, in addition to the purely algebraic properties of quaternions outlined so far, the subsequent analysis requires some kinematic identities relating quaternion derivatives to vector quantities more familiar in rigid-body dynamics. First, the time derivative of a body's attitude quaternion is related to its angular velocity in the following way:

$$\hat{\boldsymbol{\omega}} = 2 q^\dagger \dot{q} \tag{9}$$

Second, the quaternion generalized force corresponding to a torque on the body is [13,14]

$$\boldsymbol{F} = 2 q \hat{\boldsymbol{\tau}} \tag{10}$$

Schaub and Junkins provide a thorough discussion of rigid-body dynamics using quaternions [15].

III. Euler's Equation from Hamilton's Principle

This section presents a detailed derivation of the classical Euler equation using Hamilton's principle. Although the results are not new, the techniques used provide the foundation for the development of the variational integrators in the following sections. A more in-depth treatment of variational mechanics on Lie groups, including the rotation group SO(3), is given by Holm [16].

The derivation begins with the Lagrangian for a free rigid body, which, in the absence of a potential, is simply its kinetic energy:

$$L = \frac{1}{2} \boldsymbol{\omega} \cdot I \cdot \boldsymbol{\omega} = \frac{1}{2} \hat{\boldsymbol{\omega}} \cdot J \cdot \hat{\boldsymbol{\omega}} \tag{11}$$

J is the following augmented inertia matrix:

$$J = \begin{bmatrix} I_{11} & I_{12} & I_{13} & 0 \\ I_{21} & I_{22} & I_{23} & 0 \\ I_{31} & I_{32} & I_{33} & 0 \\ 0 & 0 & 0 & 0 \end{bmatrix} \tag{12}$$

Following the standard approach in variational mechanics [17,18], an action integral is constructed and its variational derivative is taken:

$$\delta S = \delta \int_{t_0}^{t_f} \frac{1}{2} \hat{\boldsymbol{\omega}} \cdot J \cdot \hat{\boldsymbol{\omega}} \, \mathrm{d}t = 0 \tag{13}$$

At this point one must be careful to take variations of $\boldsymbol{\omega}$ in such a way that the quaternion unit-norm constraint is maintained. There are several ways of explicitly enforcing the constraint in the action integral [14,19]. An alternative is to incorporate the constraint into the variation [4,6,16]. From the fact that the exponential of a quaternion having zero scalar part is always a unit quaternion, a varied unit quaternion can be defined as

$${}^\epsilon q = q e^{\epsilon \hat{\boldsymbol{\eta}}} \tag{14}$$

where a left superscript ϵ is used to denote a varied quantity. Next, ${}^\epsilon q$ is differentiated with respect to time:

$${}^\epsilon \dot{q} = \dot{q} e^{\epsilon \hat{\boldsymbol{\eta}}} + \epsilon q e^{\epsilon \hat{\boldsymbol{\eta}}} \dot{\hat{\boldsymbol{\eta}}} \tag{15}$$

Equations (14) and (15) can be substituted into the identity in Eq. (9) to obtain the desired variation of $\boldsymbol{\omega}$, keeping in mind that only terms linear in ϵ need to be retained:

$${}^\epsilon \hat{\boldsymbol{\omega}} = 2 {}^\epsilon q^\dagger {}^\epsilon \dot{q} = e^{-\epsilon \hat{\boldsymbol{\eta}}} \hat{\boldsymbol{\omega}} e^{\epsilon \hat{\boldsymbol{\eta}}} + 2\epsilon \dot{\hat{\boldsymbol{\eta}}} \approx \hat{\boldsymbol{\omega}} + \epsilon (\hat{\boldsymbol{\omega}} \hat{\boldsymbol{\eta}} - \hat{\boldsymbol{\eta}} \hat{\boldsymbol{\omega}} + 2\dot{\hat{\boldsymbol{\eta}}}) \tag{16}$$

Using Eq. (16), the variational derivative of the action integral in Eq. (13) is

$$\delta S = \frac{\mathrm{d}}{\mathrm{d}\epsilon}\bigg|_{\epsilon=0} \int_{t_0}^{t_f} \frac{1}{2} {}^\epsilon \hat{\boldsymbol{\omega}} \cdot J \cdot {}^\epsilon \hat{\boldsymbol{\omega}} \, \mathrm{d}t = \int_{t_0}^{t_f} \hat{\boldsymbol{\omega}} \cdot J \cdot (2\hat{\boldsymbol{\omega}} \hat{\boldsymbol{\eta}} + 2\dot{\hat{\boldsymbol{\eta}}}) \, \mathrm{d}t = 0 \tag{17}$$

Following the usual procedure, integration by parts is used to eliminate $\hat{\boldsymbol{\eta}}$, noting that variations must be zero at the endpoints of the integration interval:

$$\delta S = \int_{t_0}^{t_f} 2\hat{\boldsymbol{\omega}} \cdot J \cdot \hat{\boldsymbol{\omega}} \hat{\boldsymbol{\eta}} - 2\dot{\hat{\boldsymbol{\omega}}} \cdot J \cdot \hat{\boldsymbol{\eta}} \, \mathrm{d}t = 0 \tag{18}$$

Because all of the quaternions in Eq. (18) have scalar parts equal to zero, it can be converted to vector form:

$$\delta S = \int_{t_0}^{t_f} \boldsymbol{\omega} \cdot I \cdot (\boldsymbol{\omega} \times \boldsymbol{\eta}) - \dot{\boldsymbol{\omega}} \cdot I \cdot \boldsymbol{\eta} \, \mathrm{d}t = 0 \tag{19}$$

Using the fact that cyclically permuting the factors in a scalar triple product does not change its value, Eq. (19) can be rewritten as

$$\delta S = \int_{t_0}^{t_f} \boldsymbol{\eta} \cdot [(I \cdot \boldsymbol{\omega}) \times \boldsymbol{\omega}] - \dot{\boldsymbol{\omega}} \cdot I \cdot \boldsymbol{\eta} \, \mathrm{d}t = 0 \tag{20}$$

Finally, recognizing that equality must hold for all perturbations η results in Euler's equation:

$$I \cdot \dot{\boldsymbol{\omega}} + \boldsymbol{\omega} \times I \cdot \boldsymbol{\omega} = 0 \tag{21}$$

IV. Discrete-Time Euler's Equation

This section derives an algebraic equation that is a discrete-time analogue of Euler's equation. The ideas used, collectively known as discrete mechanics, are presented in detail by Marsden and West [1]. The derivation here roughly follows that of Lee et al. [4] but uses quaternions where they have used rotation matrices.

The point of departure from classical mechanics is the action integral in Eq. (13). It is first broken into finite short segments of length h, with $t_k = t_0 + kh$:

$$S = \int_{t_0}^{t_f} \frac{1}{2} \hat{\boldsymbol{\omega}} \cdot J \cdot \hat{\boldsymbol{\omega}} \, \mathrm{d}t = \sum_{k=0}^{N-1} \int_{t_k}^{t_{k+1}} \frac{1}{2} \hat{\boldsymbol{\omega}} \cdot J \cdot \hat{\boldsymbol{\omega}} \, \mathrm{d}t \tag{22}$$

The integral of the Lagrangian over a single time step h inside the summation on the right-hand side of Eq. (22) is known as the exact discrete Lagrangian [1]:

$$L_d^E = \int_{t_k}^{t_{k+1}} \frac{1}{2} \hat{\boldsymbol{\omega}} \cdot J \cdot \hat{\boldsymbol{\omega}} \, \mathrm{d}t \tag{23}$$

The next step is to approximate L_d^E using a quadrature rule. Any quadrature rule for approximating integrals can be used for this purpose, with higher order rules generally leading to higher order variational integrators [1]. The resulting approximation is known as the discrete Lagrangian of the system. In general, different quadrature rules lead to different discrete Lagrangians. For simplicity and clarity, the rectangle rule is used here. First, a finite difference approximation of $\boldsymbol{\omega}$ is defined:

$$\hat{\boldsymbol{\omega}}_k = 2 q_k^\dagger \dot{q}_k \approx 2 q_k^\dagger \left(\frac{q_{k+1} - q_k}{h} \right) = 2 \left(\frac{f_k - 1}{h} \right) \tag{24}$$

The quaternion rotation from q_k to q_{k+1} is denoted by $f_k = q_k^\dagger q_{k+1}$. Substituting the approximation for $\hat{\boldsymbol{\omega}}_k$ into Eq. (23), applying the rectangle rule, and simplifying leads to the following discrete Lagrangian:

$$L_d = \frac{2}{h} f_k \cdot J \cdot f_k \tag{25}$$

Using Eq. (25), the discrete action sum for the system can be formed:

$$S_d = \sum_{k=0}^{N-1} L_d = \sum_{k=0}^{N-1} \frac{2}{h} f_k \cdot J \cdot f_k \tag{26}$$

Equation (26) approximates Eq. (22) and serves the same role in discrete mechanics as the action integral does in traditional variational mechanics [1]. Analogously to the continuous case, Hamilton's principle is applied to the action sum. First, a varied f_k that obeys the unit quaternion constraint is needed:

$${}^{\epsilon} f_k = {}^{\epsilon} q_k^\dagger {}^{\epsilon} q_{k+1} = e^{-\epsilon \hat{\boldsymbol{\eta}}} f_k e^{\epsilon \hat{\boldsymbol{\eta}}} \approx f_k + \epsilon (f_k \hat{\boldsymbol{\eta}}_{k+1} - \hat{\boldsymbol{\eta}}_k f_k) \tag{27}$$

Using ${}^{\epsilon} f_k$, the variation of the action sum is set equal to zero:

$$\begin{aligned} \delta S_d &= \left. \frac{\mathrm{d}}{\mathrm{d}\epsilon} \right|_{\epsilon=0} \sum_{k=0}^{N-1} \frac{2}{h} {}^{\epsilon} f k \cdot J \cdot {}^{\epsilon} f_k \\ &= \sum_{k=0}^{N-1} \frac{4}{h} f_k \cdot J \cdot (f_k \hat{\boldsymbol{\eta}}_{k+1} - \hat{\boldsymbol{\eta}}_k f_k) = 0 \end{aligned} \tag{28}$$

The next step is to eliminate $\boldsymbol{\eta}_{k+1}$ from the right-hand side of Eq. (28) by performing the discrete equivalent of integration by parts, which amounts to some simple index manipulation:

$$\begin{aligned} \delta S_d = {} & f_{N-1} \cdot J \cdot f_{N-1} \hat{\boldsymbol{\eta}}_N - f_0 \cdot J \cdot f_0 \hat{\boldsymbol{\eta}}_0 \\ & + \sum_{k=1}^{N-1} \frac{4}{h} f_{k-1} \cdot J \cdot (f_{k-1} \hat{\boldsymbol{\eta}}_k - \hat{\boldsymbol{\eta}}_k f_k) = 0 \end{aligned} \tag{29}$$

Using the fact that variations at the endpoints must be zero, just as in the continuous case, the first two terms in Eq. (29) can be eliminated:

$$\delta S_d = \sum_{k=1}^{N-1} \frac{4}{h} f_{k-1} \cdot J \cdot (f_{k-1} \hat{\boldsymbol{\eta}}_k - \hat{\boldsymbol{\eta}}_k f_k) = 0 \tag{30}$$

At this point, Eq. (30), which implicitly includes unit-norm constraints on the quaternions, is converted to an unconstrained vector equation by parameterizing f_k in the following way:

$$f_k = \begin{bmatrix} \boldsymbol{\phi}_k \\ \sqrt{1 - \boldsymbol{\phi}_k \cdot \boldsymbol{\phi}_k} \end{bmatrix} \tag{31}$$

This parameterization is only valid for $|\boldsymbol{\phi}_k| < 1$. Therefore, h must be chosen small enough to ensure that the incremental rotations between adjacent time steps are less than 180 deg. A number of other three-parameter attitude representations could be used instead (modified Rodrigues parameters, for example), however, Eq. (31) is a natural choice that leads to simple and elegant expressions.

In terms of $\boldsymbol{\phi}_k$, Eq. (30) is

$$\begin{aligned} \sum_{k=1}^{N-1} [& \sqrt{1 - \boldsymbol{\phi}_k \cdot \boldsymbol{\phi}_k} \boldsymbol{\eta}_k \cdot I \cdot \boldsymbol{\phi}_k - \boldsymbol{\phi}_k \cdot I \cdot (\boldsymbol{\phi}_k \times \boldsymbol{\eta}_k) \\ & - \sqrt{1 - \boldsymbol{\phi}_{k-1} \cdot \boldsymbol{\phi}_{k-1}} \boldsymbol{\eta}_k \cdot I \cdot \boldsymbol{\phi}_{k-1} - \boldsymbol{\phi}_{k-1} \cdot I \cdot (\boldsymbol{\phi}_{k-1} \times \boldsymbol{\eta}_k)] = 0 \end{aligned} \tag{32}$$

Recognizing that Eq. (32) must be true for all $\boldsymbol{\eta}_k$ and performing some simple vector algebra reveals an algebraic equation relating the incremental rotation from the last time step to the current time step $\boldsymbol{\phi}_k$ to the incremental rotation from the current time step to the next time step $\boldsymbol{\phi}_{k+1}$:

$$\begin{aligned} & \sqrt{1 - \boldsymbol{\phi}_k \cdot \boldsymbol{\phi}_k} I \cdot \boldsymbol{\phi}_k - \boldsymbol{\phi}_k \times I \cdot \boldsymbol{\phi}_k \\ & \quad = \sqrt{1 - \boldsymbol{\phi}_{k+1} \cdot \boldsymbol{\phi}_{k+1}} I \cdot \boldsymbol{\phi}_{k+1} + \boldsymbol{\phi}_{k+1} \times I \cdot \boldsymbol{\phi}_{k+1} \end{aligned} \tag{33}$$

As a brief aside, Eq. (33) bears some resemblance to the classical Euler's equation. Taking its limit as h goes to zero does, in fact, recover Eq. (21). This result confirms that the discrete-time equation converges to the true differential equation for small time steps and establishes consistency with the continuous theory.

V. Variational Integrator for the Free Rigid Body

This section uses Eq. (33) as the starting point for the development of a variational integrator for the unforced rigid body. The additional ingredients needed are a way to initialize the integrator given an attitude q_0 and angular velocity $\boldsymbol{\omega}_0$, a way to update the attitude q_{k+1} and angular velocity $\boldsymbol{\omega}_{k+1}$ after solving for $\boldsymbol{\phi}_{k+1}$, and a way to solve Eq. (33) for $\boldsymbol{\phi}_{k+1}$ given $\boldsymbol{\phi}_k$.

Although it might seem simple enough to approximate $\boldsymbol{\phi}_0$ in any number of ways given $\boldsymbol{\omega}_0$, ad hoc approaches do not maintain the

variational integrator's conservation properties. The discrete Legendre transform [1] gives a consistent way to convert between $\boldsymbol{\phi}_k$ and $\boldsymbol{\omega}_k$. Similar to the classical Legendre transform [17], it maps from $\boldsymbol{\phi}_k$ (which is effectively the discrete-time velocity variable) to $\boldsymbol{p}_k$, the momentum at time k, which can then be multiplied by I^{-1} to recover $\boldsymbol{\omega}_k$. Unlike the continuous version, there are actually two discrete Legendre transforms for a given time step [1]:

$$\boldsymbol{p}_k^- = -\frac{\partial L_d(q_k, q_{k+1})}{\partial q_k} \cdot \delta q_k \tag{34}$$

$$\boldsymbol{p}_k^+ = \frac{\partial L_d(q_k, q_{k+1})}{\partial q_{k+1}} \cdot \delta q_{k+1} \tag{35}$$

Applying these transformations to the discrete Lagrangian in Eq. (25) reveals that $\boldsymbol{p}_k^-$ and $\boldsymbol{p}_k^+$ correspond to the left and right sides of Eq. (33):

$$\boldsymbol{p}_k^- = \frac{2}{h}\sqrt{1-\boldsymbol{\phi}_k\cdot\boldsymbol{\phi}_k}I\cdot\boldsymbol{\phi}_k - \boldsymbol{\phi}_k \times I\cdot\boldsymbol{\phi}_k \tag{36}$$

$$\boldsymbol{p}_k^+ = \frac{2}{h}\sqrt{1-\boldsymbol{\phi}_{k+1}\cdot\boldsymbol{\phi}_{k+1}}I\cdot\boldsymbol{\phi}_{k+1} + \boldsymbol{\phi}_{k+1} \times I\cdot\boldsymbol{\phi}_{k+1} \tag{37}$$

This result leads to several key conclusions. First, Eqs. (36) and (37) provide a new interpretation of the discrete-time equation of motion as a momentum balance between adjacent time steps. Second, Eq. (36) can be used to initialize the integrator by solving for $\boldsymbol{\phi}_0$ given I and $\boldsymbol{\omega}_0$. Lastly, $\boldsymbol{p}_k$, and hence $\boldsymbol{\omega}_k$, can be calculated at any point during the integration using either Eqs. (36) or (37).

The final missing piece of the integrator is a method for solving Eq. (33), which is both implicit and nonlinear. Newton's method, which amounts to solving successive linear approximations of the equation until a desired level of accuracy is achieved [3,20], provides an efficient solution in this case. The necessary linear approximation is the Jacobian matrix of Eq. (37),

$$\frac{\partial \boldsymbol{p}_k}{\partial \boldsymbol{\phi}_{k+1}} = \frac{2}{h}\left[\sqrt{1-\boldsymbol{\phi}_{k+1}^\top\boldsymbol{\phi}_{k+1}}I - \frac{I\boldsymbol{\phi}_{k+1}\boldsymbol{\phi}_{k+1}^\top}{\sqrt{1-\boldsymbol{\phi}_{k+1}^\top\boldsymbol{\phi}_{k+1}}} + \operatorname{skew}(\boldsymbol{\phi}_{k+1})I - \operatorname{skew}(I\boldsymbol{\phi}_{k+1})\right] \tag{38}$$

where $\operatorname{skew}(\boldsymbol{\phi})$ indicates the skew-symmetric matrix-multiplication equivalent of the cross-product operation:

$$\operatorname{skew}\left(\begin{bmatrix}\boldsymbol{\phi}_1\\ \boldsymbol{\phi}_2\\ \boldsymbol{\phi}_3\end{bmatrix}\right) = \begin{bmatrix}0 & -\boldsymbol{\phi}_3 & \boldsymbol{\phi}_2\\ \boldsymbol{\phi}_3 & 0 & -\boldsymbol{\phi}_1\\ -\boldsymbol{\phi}_2 & \boldsymbol{\phi}_1 & 0\end{bmatrix} \tag{39}$$

Three or four Newton iterations are sufficient to reach machine precision in all of the examples presented in Sec. IX using standard 64 bit floating-point arithmetic. Once $\boldsymbol{\phi}_{k+1}$ is computed, the attitude can be updated by simple quaternion multiplication with the previous attitude $q_{k+1} = q_k f_k$.

In summary, given an inertia I and initial conditions q_0 and $\boldsymbol{\omega}_0$, the integrator is initialized by computing the momentum $\boldsymbol{p}_0 = I\cdot\boldsymbol{\omega}_0$ and an initial guess for $\boldsymbol{\phi}_0$. A reasonable guess is

$$\boldsymbol{\phi}_0 \approx \frac{h}{2}\boldsymbol{\omega}_0$$

The true value of $\boldsymbol{\phi}_0$ is then calculated to machine precision using Newton's method with Eqs. (37) and (38). From $\boldsymbol{\phi}_0$, $\boldsymbol{p}_1$ is calculated using Eq. (36), followed by $\boldsymbol{\omega}_1$ and q_1. The process is then repeated as desired.

VI. Gyrostats

A gyrostat is a system of coupled rigid bodies whose relative motions do not change the total inertia tensor of the system [21]. A practical example is a rigid body with internal rotors or momentum actuators that can spin relative to the carrier body, such as a spacecraft with reaction wheels. Using the variational framework developed in the preceding sections, both the classical equations of motion and a variational integrator are straightforward to derive.

The Lagrangian for a gyrostat system is

$$L = \frac{1}{2}\boldsymbol{\omega}_B\cdot I_B\cdot\boldsymbol{\omega}_B + \sum_{r=1}^{N}\frac{1}{2}(\boldsymbol{\omega}_B+\boldsymbol{\omega}_r)\cdot I_r\cdot(\boldsymbol{\omega}_B+\boldsymbol{\omega}_r) + \frac{1}{2}m_r(\boldsymbol{\omega}_B\times\boldsymbol{x}_r)^2 \tag{40}$$

where I_B and $\boldsymbol{\omega}_B$ are the carrier body's inertia tensor and angular velocity, the I_r are the rotor inertia tensors, the $\boldsymbol{\omega}_r$ are the rotor angular velocities relative to the carrier body, and the $\boldsymbol{x}_r$ are the rotor positions relative to the carrier body's center of mass. The Lagrangian can be simplified by introducing a modified body inertia I_B', which includes the rotor masses:

$$I_B' = I_B - \sum_{r=0}^{N} m_r\operatorname{skew}(\boldsymbol{x}_r)^2 \tag{41}$$

Substituting I_B' into Eq. (40) eliminates the last term, giving the simpler expression

$$L = \frac{1}{2}\boldsymbol{\omega}_B\cdot I_B'\cdot\boldsymbol{\omega}_B + \sum_{r=1}^{N}\frac{1}{2}(\boldsymbol{\omega}_B+\boldsymbol{\omega}_r)\cdot I_r\cdot(\boldsymbol{\omega}_B+\boldsymbol{\omega}_r) \tag{42}$$

The rotor angular velocities $\boldsymbol{\omega}_r$ are treated as exogenous inputs to the system that can be set arbitrarily (e.g., by a controller), and so variations need only be taken with respect to $\boldsymbol{\omega}_B$. This fact makes the derivation for the gyrostat nearly identical to the free rigid body. The only difference is that a few extra terms involving I_r and $\boldsymbol{\omega}_r$ are carried through. Using ${}^e\boldsymbol{\omega}_B$ to vary the action and following the rest of the steps in Sec. III results in the following differential equation:

$$I_B'\cdot\dot{\boldsymbol{\omega}}_B + \boldsymbol{\omega}_B\times I_B'\cdot\boldsymbol{\omega}_B + \sum_{r=1}^{N} I_r\cdot\dot{\boldsymbol{\omega}}_B + \boldsymbol{\omega}_B\times I_r\cdot\boldsymbol{\omega}_B + I_r\cdot\dot{\boldsymbol{\omega}}_r + \boldsymbol{\omega}_B\times I_r\cdot\boldsymbol{\omega}_r = 0 \tag{43}$$

Two new definitions help simplify Eq. (43). First, the gyrostat inertia I_G is

$$I_G = I_B' + \sum_{r=0}^{N} I_r = I_B + \sum_{r=0}^{N} I_r - m_r\operatorname{skew}(\boldsymbol{x}_r)^2 \tag{44}$$

Second, $\boldsymbol{\rho}$ is the total angular momentum stored in all the rotors:

$$\boldsymbol{\rho} = \sum_{r=0}^{N} I_r\cdot\boldsymbol{\omega}_r \tag{45}$$

Substituting I_G and $\boldsymbol{\rho}$ into Eq. (43) results in the classical equation of motion for the gyrostat [21]:

$$I_G\cdot\dot{\boldsymbol{\omega}}_B + \boldsymbol{\omega}_B\times(I_G\cdot\boldsymbol{\omega}_B+\boldsymbol{\rho}) + \dot{\boldsymbol{\rho}} = 0 \tag{46}$$

The steps involved in deriving the discrete-time equivalent of Eq. (46) are now briefly highlighted. If $\boldsymbol{\omega}_B$ is approximated as in Eq. (24) and the rectangle rule is used, the discrete Lagrangian for the gyrostat is

$$L_d = \frac{2}{h}[f_k \cdot J'_B \cdot f_k + \sum_{r=1}^{N}\left(f_k + \frac{h}{2}\hat{\boldsymbol{\omega}}_{r,k}\right) \cdot J_r \cdot \left(f_k + \frac{h}{2}\hat{\boldsymbol{\omega}}_{r,k}\right)] \tag{47}$$

where J'_B and J_r are the augmented 4×4 equivalents of I'_B and I_r. The discrete action sum S_d can then be formed as in Eq. (26) and its variation taken using ${}^{\epsilon}f_k$ from Eq. (27):

$$\delta\mathcal{S}_d = \sum_{k=0}^{N-1}[f_k \cdot J_B \cdot (f_k\hat{\boldsymbol{\eta}}_{k+1} - \hat{\boldsymbol{\eta}}_k f_k) + \sum_{r=1}^{N}\left(f_k + \frac{h}{2}\hat{\boldsymbol{\omega}}_{r,k}\right) \cdot J_r \cdot (f_k\hat{\boldsymbol{\eta}}_{k+1} - \hat{\boldsymbol{\eta}}_k f_k)] = 0 \tag{48}$$

Following the rest of the steps in Sec. IV and substituting in I_G and $\boldsymbol{\rho}$ results in the discrete-time gyrostat equation:

$$\sqrt{1-\boldsymbol{\phi}_k\cdot\boldsymbol{\phi}_k}\left(I_G\cdot\boldsymbol{\phi}_k + \frac{h}{2}\boldsymbol{\rho}_k\right) - \boldsymbol{\phi}_k \times \left(I_G\cdot\boldsymbol{\phi}_k + \frac{h}{2}\boldsymbol{\rho}_k\right) = \sqrt{1-\boldsymbol{\phi}_{k+1}\cdot\boldsymbol{\phi}_{k+1}}\left(I_G\cdot\boldsymbol{\phi}_{k+1} + \frac{h}{2}\boldsymbol{\rho}_{k+1}\right) + \boldsymbol{\phi}_{k+1} \times \left(I_G\cdot\boldsymbol{\phi}_{k+1} + \frac{h}{2}\boldsymbol{\rho}_{k+1}\right) \tag{49}$$

Equation (49) can be directly substituted into the variational integrator developed in Sec. V. The only other change necessary is to the Jacobian in the Newton iteration:

$$\frac{\partial \boldsymbol{p}^+}{\partial \boldsymbol{\phi}_{k+1}} = \frac{2}{h}[\sqrt{1-\boldsymbol{\phi}^\top\boldsymbol{\phi}}I - \frac{I\boldsymbol{\phi}\boldsymbol{\phi}^\top}{\sqrt{1-\boldsymbol{\phi}^\top\boldsymbol{\phi}}} + \text{skew}(\boldsymbol{\phi})I - \text{skew}(I\boldsymbol{\phi}) - \frac{h}{2}\frac{\boldsymbol{\rho}\boldsymbol{\phi}^\top}{\sqrt{1-\boldsymbol{\phi}^\top\boldsymbol{\phi}}} - \frac{h}{2}\text{skew}(\boldsymbol{\rho})] \tag{50}$$

VII. External Torques

External torques can be incorporated into the variational framework using the Lagrange–d'Alembert principle (often known simply as d'Alembert's principle) [17,18]. In particular, its integral form [1,22]

$$\delta\int_{t_0}^{t_f} L\,\mathrm{d}t + \int_{t_0}^{t_f} \boldsymbol{F}\cdot\delta q\,\mathrm{d}t = 0 \tag{51}$$

is most readily applied here, where the term on the left is simply the variation of the action δS and the term on the right is the integral of the virtual work done by a generalized force $\boldsymbol{F}$.

To apply the Lagrange–d'Alembert principle to a rigid body, the expression for the quaternion generalized force given in Eq. (10), as well as the variational derivative of the attitude quaternion δq, are substituted into the second term of Eq. (51):

$$\int_{t_0}^{t_f} \boldsymbol{F}\cdot\delta q\,\mathrm{d}t = \int_{t_0}^{t_f} 2q\hat{\boldsymbol{\tau}}\cdot(q\hat{\boldsymbol{\eta}})\,\mathrm{d}t \tag{52}$$

A little algebra reveals that $(q\hat{\boldsymbol{\tau}})\cdot(q\hat{\boldsymbol{\eta}}) = \boldsymbol{\tau}\cdot\boldsymbol{\eta}$, further simplifying the expression. Combining this result with the action term from Eq. (18) leads to the following equation:

$$\int_{t_0}^{t_f} 2\hat{\boldsymbol{\omega}}\cdot J\cdot\hat{\boldsymbol{\omega}}\,\hat{\boldsymbol{\eta}} - 2\dot{\hat{\boldsymbol{\omega}}}\cdot J\cdot\hat{\boldsymbol{\eta}} + 2\hat{\boldsymbol{\tau}}\cdot\hat{\boldsymbol{\eta}}\,\mathrm{d}t = 0 \tag{53}$$

It is then straightforward to work through the rest of the steps in Sec. III to arrive at the forced Euler equation:

$$I\cdot\dot{\boldsymbol{\omega}} + \boldsymbol{\omega}\times I\cdot\boldsymbol{\omega} = \boldsymbol{\tau} \tag{54}$$

Incorporating forcing into the discrete variational framework is a bit more subtle than in the continuous case. The discrete version of the Lagrange–d'Alembert principle is

$$\delta\sum_{k=0}^{N} L_d + \sum_{k=0}^{N} \boldsymbol{F}_d^- \cdot \delta q_k + \boldsymbol{F}_d^+ \cdot \delta q_{k+1} = 0 \tag{55}$$

where $\boldsymbol{F}_d^-$ and $\boldsymbol{F}_d^+$ are known as discrete generalized forces [1]. Similar to what is encountered with the discrete Legendre transform, there are two discrete generalized forces corresponding to the beginning and end of a time step:

$$\boldsymbol{F}_d^- = \int_{t_k}^{t_{k+1}} \frac{1}{2}\boldsymbol{F}(q,\dot{q})\cdot\frac{\partial q(t)}{\partial q_k}\,\mathrm{d}t \tag{56}$$

$$\boldsymbol{F}_d^+ = \int_{t_k}^{t_{k+1}} \frac{1}{2}\boldsymbol{F}(q,\dot{q})\cdot\frac{\partial q(t)}{\partial q_{k+1}}\,\mathrm{d}t \tag{57}$$

As with the discrete Lagrangian, the integrals in the definition of the discrete generalized forces are approximated by quadrature. Here, the rectangle rule is used, though more accurate quadrature rules can lead to more accurate integrators at the expense of increased computational burden:

$$\boldsymbol{F}_d^- \approx hq_k\hat{\boldsymbol{\tau}}_k \tag{58}$$

$$\boldsymbol{F}_d^+ \approx hq_{k+1}\hat{\boldsymbol{\tau}}_{k+1} \tag{59}$$

Substituting the approximations for $\boldsymbol{F}_d^-$ and $\boldsymbol{F}_d^+$, as well as the discrete Lagrangian for the rigid body from Eq. (25), into Eq. (55) results in

$$\delta\sum_{k=0}^{N}\frac{2}{h}f_k\cdot J\cdot f_k + \sum_{k=0}^{N} hq_k\hat{\boldsymbol{\tau}}_k\cdot\delta q_k + hq_{k+1}\hat{\boldsymbol{\tau}}_{k+1}\cdot\delta q_{k+1} = 0 \tag{60}$$

Carrying out the variational derivatives leads to the following:

$$\sum_{k=0}^{N}\frac{4}{h}f_k\cdot J\cdot(f_k\boldsymbol{\eta}_{k+1} - \boldsymbol{\eta}_k f_k) + h\hat{\boldsymbol{\tau}}_k\cdot\hat{\boldsymbol{\eta}}_k + h\hat{\boldsymbol{\tau}}_{k+1}\cdot\hat{\boldsymbol{\eta}}_{k+1} = 0 \tag{61}$$

Eliminating the $\boldsymbol{\eta}_{k+1}$ terms again requires a "discrete integration by parts." Manipulating indices results in

$$\sum_{k=1}^{N}\frac{4}{h}f_{k-1}\cdot J\cdot(f_{k-1}\boldsymbol{\eta}_k - \boldsymbol{\eta}_k f_k) + 2h\hat{\boldsymbol{\tau}}_k\cdot\hat{\boldsymbol{\eta}}_k = 0 \tag{62}$$

Retracing the remaining steps in Sec. IV yields the discrete-time equation of motion for the forced rigid body:

$$\sqrt{1-\boldsymbol{\phi}_k\cdot\boldsymbol{\phi}_k}I\cdot\boldsymbol{\phi}_k - \boldsymbol{\phi}_k\times I\cdot\boldsymbol{\phi}_k = \sqrt{1-\boldsymbol{\phi}_{k+1}\cdot\boldsymbol{\phi}_{k+1}}I\cdot\boldsymbol{\phi}_{k+1} + \boldsymbol{\phi}_{k+1}\times I\cdot\boldsymbol{\phi}_{k+1} + \frac{h^2}{2}\boldsymbol{\tau}_{k+1} \tag{63}$$

This result can also be readily applied to the forced gyrostat by adding the same torque term onto the right-hand side of Eq. (49).

VIII. Gyrostat Spacecraft with Damping

The tools developed up to this point enable the construction of a variational integrator for a gyrostat with an internal energy-dissipating mechanism. The mechanism considered here is known as a Kane damper and consists of a spherical mass immersed in a viscous fluid inside a spherical cavity in the spacecraft body [23]. The torque exerted on the spacecraft by the damper is

$$\boldsymbol{\tau} = C(\boldsymbol{\omega}_D - \boldsymbol{\omega}_B) \tag{64}$$

where C is a damping constant, $\boldsymbol{\omega}_D$ is the damper angular velocity, and $\boldsymbol{\omega}_B$ is the body angular velocity.

The basic approach taken here is to treat the body and damper as separate rigid bodies coupled through the viscous damping force. Equation (64) is approximated by finite differences in the usual way, giving

$$\boldsymbol{\tau}_k \approx \frac{2}{h} C(\boldsymbol{\gamma}_k - \boldsymbol{\phi}_k) \tag{65}$$

where $\boldsymbol{\phi}_k$ is the incremental body rotation defined in Eq. (31) and $\boldsymbol{\gamma}_k$ is the analogous incremental rotation for the damper. Substituting this approximation into Eq. (63) yields a set of coupled equations for the gyrostat–damper system:

$$\begin{aligned}
&\sqrt{1-\boldsymbol{\phi}_k\cdot\boldsymbol{\phi}_k}\left(I_G\cdot\boldsymbol{\phi}_k+\frac{h}{2}\boldsymbol{\rho}_k\right)-\boldsymbol{\phi}_k\times\left(I_G\cdot\boldsymbol{\phi}_k+\frac{h}{2}\boldsymbol{\rho}_k\right)\\
&\quad=\sqrt{1-\boldsymbol{\phi}_{k+1}\cdot\boldsymbol{\phi}_{k+1}}\left(I_G\cdot\boldsymbol{\phi}_{k+1}+\frac{h}{2}\boldsymbol{\rho}_{k+1}\right)+\boldsymbol{\phi}_{k+1}\\
&\quad\times\left(I_G\cdot\boldsymbol{\phi}_{k+1}+\frac{h}{2}\boldsymbol{\rho}_{k+1}\right)+hC(\boldsymbol{\gamma}_{k+1}-\boldsymbol{\phi}_{k+1})
\end{aligned} \tag{66}$$

$$\sqrt{1-\boldsymbol{\gamma}_k\cdot\boldsymbol{\gamma}_k}I_D=\sqrt{1-\boldsymbol{\gamma}_{k+1}\cdot\boldsymbol{\gamma}_{k+1}}I_D\cdot\boldsymbol{\gamma}_{k+1}-hC(\boldsymbol{\gamma}_{k+1}-\boldsymbol{\phi}_{k+1}) \tag{67}$$

These equations take advantage of the fact that the damper is spherical, and thus has an inertia tensor that is a scalar multiple of the identity, to eliminate the cross-product term in Eq. (67).

Equations (66) and (67) must be solved simultaneously for $\boldsymbol{\phi}_{k+1}$ and $\boldsymbol{\gamma}_{k+1}$. Once again, Newton's method is used, this time with both equations combined to form a single six-dimensional system. The necessary 6×6 Jacobian matrix is easily derived in terms of Eqs. (38) and (50). In addition to the steps outlined in Sec. V, a subtlety arises in the implementation of this integrator in that the components of the damper's angular-momentum vector must be rotated by f_k at the end of each time step to keep them aligned with the spacecraft body frame.

IX. Numerical Examples

This section presents some numerical examples to demonstrate the performance of the variational integrators derived in Secs. IV–VIII. Comparisons are made to the second-order fixed-step midpoint rule and MATLAB's ODE45 and ODE15s variable-step Runge–Kutta solvers with default error tolerances [24]. The computational cost of the midpoint rule roughly equals that of the variational integrators. In all simulations, the following inertia matrix is used:

$$I=\begin{bmatrix}1&0&0\\0&2&0\\0&0&3\end{bmatrix} \tag{68}$$

A. Free Rigid Body

The first test compares the energy and momentum behavior of the integrator in Sec. V with the midpoint rule and ODE45 by simulating a free rigid body with an initial angular velocity $\boldsymbol{\omega}_0 = [\pi/4, -\pi/5, \pi/6]^T$ rad/s. The time steps for the midpoint rule and the variational integrator are chosen to be $h = 0.2$ s to make the run time for both roughly equal to that of ODE45. Because this system is conservative, both the inertial angular-momentum vector components and the total energy should remain constant throughout the simulation.

Figure 1 shows the normalized momentum error magnitude for all three integrators, and Fig. 2 shows the normalized energy error. Figure 3 shows these errors for the variational integrator after continuing the simulation for one million time steps. Together, all three demonstrate the excellent conservation properties and long-term stability of the variational integrator. The gradual accumulation of error shown in Fig. 3 is due to numerical roundoff and is an unavoidable consequence of using finite-precision floating-point arithmetic.

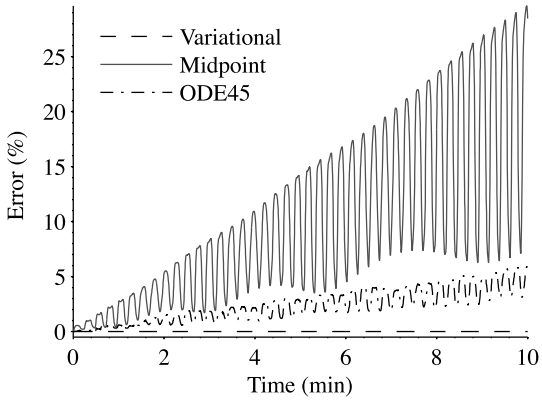

Fig. 1 Momentum error for a free rigid body.

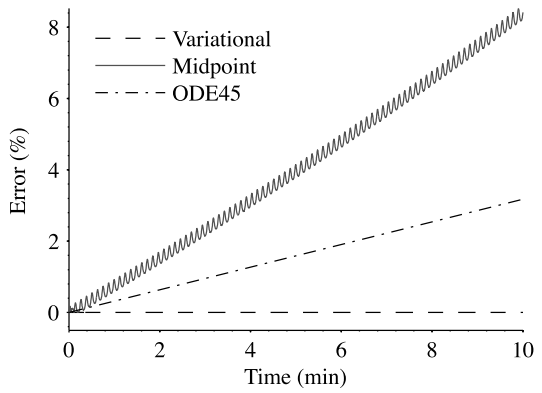

Fig. 2 Energy error for a free rigid body.

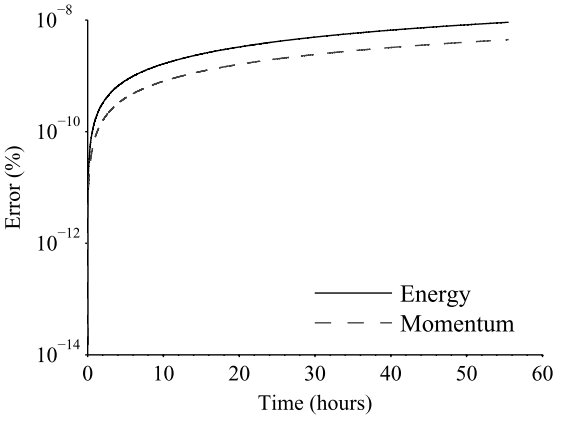

Fig. 3 Long-term error for a free rigid body.

Although it is possible to achieve better momentum and energy conservation with traditional integrators by using smaller time steps and higher order methods, doing so can become prohibitively computationally expensive for long integration times. The energy and momentum behavior of the variational integrator produces qualitatively realistic simulation results in cases where traditional integrators can produce unphysical behavior.

B. Damped Rigid Body

The second test incorporates the spherical damper of Sec. VIII into the rigid-body simulation. The damper inertia is set to $I_D = 0.2$ and the damping constant C is varied from 0.1 to 100. The midpoint rule is not shown because it quickly diverges as C is increased and requires extremely small step sizes to avoid divergence.

Figure 4 shows the running time of ODE45 with default error tolerances and the variational integrator with a step size of $h = 0.3$ s, which is chosen so that the running times are roughly equal for small values of C. As the damping constant increases, the magnitude of the forces between the body and the damper increase and ODE45 must shorten its time steps to maintain accuracy and avoid diverging. The variational integrator, on the other hand, remains stable with a relatively large fixed step size.

Figure 5 shows the total energy of the system over the course of a simulation with $C = 100$. The variational integrator shows essentially the same energy damping behavior as ODE45 on this dissipative system while running over 50 times faster. Figure 6 shows the same simulation again, but with MATLAB's ODE15s solver, which is intended for solving stiff systems, substituted for ODE45. The ODE15s solver runs in roughly the same time as the variational integrator on this problem but produces obviously incorrect and unrealistic energy behavior, with the total energy increasing over time.

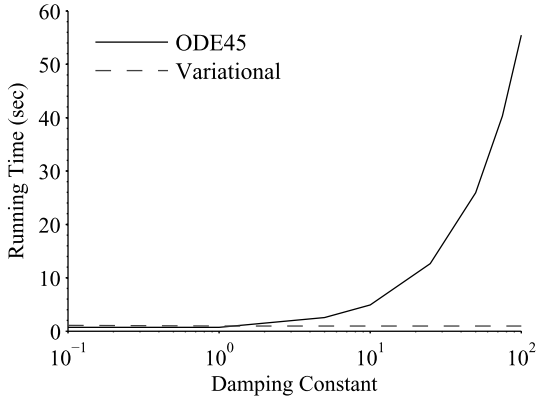

Fig. 4 Integrator running time.

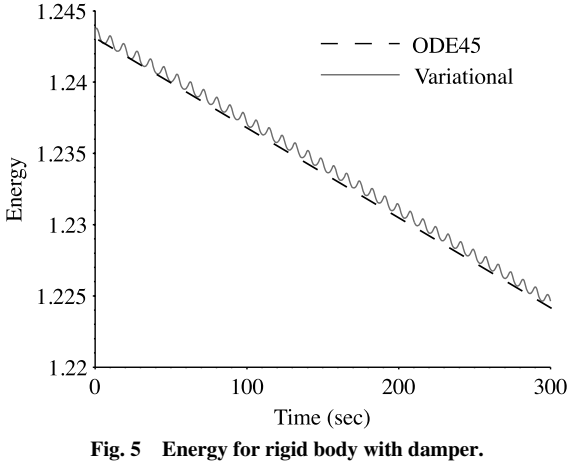

Fig. 5 Energy for rigid body with damper.

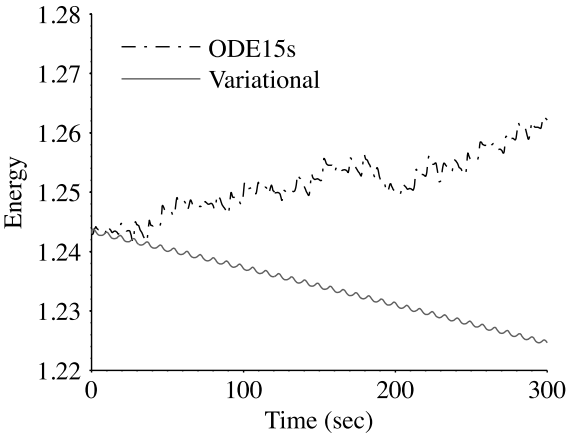

Fig. 6 Energy for rigid body with damper.

C. Extended Kalman Filter

The final test case demonstrates the advantages of variational integrators in a real-time estimation application. A spacecraft attitude determination problem is simulated where a multiplicative extended Kalman filter (MEKF) [25,26] is used to estimate the attitude quaternion from noisy measurements of two inertial reference vectors. This situation is typical on CubeSats, for example, where magnetometer and sun vector measurements are commonly used for attitude determination.

A simulated truth model is constructed by integrating the rigid-body equations of motion with initial conditions $q_0 = [0, 0, 0, 1]^T$ and $\boldsymbol{\omega}_0 = [4, -5, 6]^T$ deg/s using ODE45 in MATLAB. Simulated vector measurements are then generated and Gaussian noise is added. Attitudes for filter initialization are computed from the first pair of noisy measurement vectors using the triad of vectors (TRIAD) algorithm [27].

Figure 7 compares a standard MEKF to one using a variational integrator to perform its state prediction step. The two filters have nearly identical performance at high sample rates but show very different behaviors as the sample rate decreases. The underlying reason for this performance difference is the quality of the linearizations that the variational integrator yields. Equation (38) and the corresponding Jacobian of Eq. (36) lead to the true linearization of the map from $\boldsymbol{\phi}_k$ to $\boldsymbol{\phi}_{k+1}$:

$$\frac{\partial \boldsymbol{\phi}_{k+1}}{\partial \boldsymbol{\phi}_k} = \left(\frac{\partial \boldsymbol{p}_k}{\partial \boldsymbol{\phi}_{k+1}}\right)^{-1} \frac{\partial \boldsymbol{p}_k}{\partial \boldsymbol{\phi}_k} \tag{69}$$

This linearization is completely independent of the step size taken. As a result, filters built around variational integrators are highly insensitive to sample rate and can maintain good performance and convergence at much lower rates than standard extended Kalman filters.

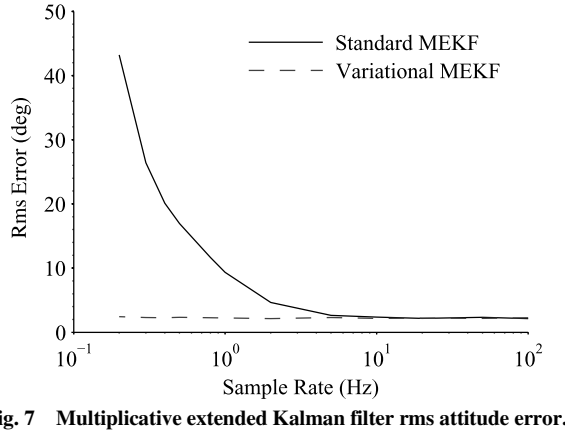

Fig. 7 Multiplicative extended Kalman filter rms attitude error.

X. Conclusions

The integrators developed in this study offer physically realistic momentum and energy behavior while having modest computational costs. They consistently outperform Runge–Kutta schemes in a variety of tests on both conservative and nonconservative systems. High-quality linearizations can also be computed as part of the integration process, making the algorithms well suited for use in real-time estimation and control applications like attitude filtering. Lastly, the methods introduced are general and can be used to develop variational integrators for a wide range of applications in spacecraft dynamics.

References

[1] Marsden, J. E., and West, M., "Discrete Mechanics and Variational Integrators," *Acta Numerica*, Vol. 10, May 2001, pp. 357–514. doi:10.1017/S096249290100006X

[2] Hairer, E., Lubich, C., and Wanner, G., "Geometric Numerical Integration Illustrated by the Störmer-Verlet method," *Acta Numerica*, Vol. 12, May 2003, pp. 399–450. doi:10.1017/S0962492902000144

[3] Press, W., Teukolsky, S., Vetterling, W., and Flannery, B., *Numerical Recipes: The Art of Scientific Computing*, 3rd ed., Cambridge Univ. Press, Cambridge, England, U.K., 2007, pp. 473–476, 928–931.

[4] Lee, T., McClamroch, N., and Leok, M., "Lie Group Variational Integrator for the Attitude Dynamics of a Rigid Body with Applications to the 3D Pendulum," *Proceedings of the 2005 IEEE Conference on Control Applications*, IEEE Publ., Piscataway, NJ, 2005, pp. 962–967. doi:10.1109/CCA.2005.1507254

[5] Lee, T., Leok, M., and McClamroch, N. H., "Lie Group Variational Integrators for the Full Body Problem in Orbital Mechanics," *Celestial Mechanics and Dynamical Astronomy*, Vol. 98, No. 2, 2007, pp. 121–144. doi:10.1007/s10569-007-9073-x

[6] Hussein, I., Leok, M., Sanyal, A., and Bloch, A., "Discrete Variational Integrator for Optimal Control Problems on SO(3)," *Proceedings of the 45th IEEE Conference on Decision and Control*, IEEE Publ., Piscataway, NJ, 2006, pp. 6636–6641. doi:10.1109/CDC.2006.377818

[7] Barth, E., and Leimkuhler, B., "Symplectic Methods for Conservative Multibody Systems," *Integration Algorithms and Classical Mechanics*, edited by Marsden, J. E., Patrick, G. W., and Shadwick, W. F., Vol. 10, Fields Inst. Communications, American Mathematical Soc., Providence, RI, 1999, pp. 25–43.

[8] McLachlan, R. I., "Explicit Lie-Poisson Integration and the Euler Equations," *Physical Review Letters*, Vol. 71, No. 19, 1993, pp. 3043–3046. doi:10.1103/PhysRevLett.71.3043

[9] Omelyan, I. P., "Algorithm for Numerical Integration of the Rigid-Body Equations of Motion," *Physical Review E: Statistical, Nonlinear, and Soft Matter Physics*, Vol. 58, No. 1, 1998, p. 1169. doi:10.1103/PhysRevE.58.1169

[10] Omelyan, I. P., "On the Numerical Integration of Motion for Rigid Polyatomics: The Modified Quaternion Approach," *Computers in Physics*, Vol. 12, No. 1, 1998, pp. 97–103. doi:10.1063/1.168642

[11] Krysl, P., "Direct Time Integration of Rigid Body Motion with Discrete-Impulse Midpoint Approximation: Explicit Newmark Algorithms," *Communications in Numerical Methods in Engineering*, Vol. 22, No. 5, 2006, pp. 441–451. doi:10.1002/cnm.826

[12] Altmann, S., *Rotations, Quaternions, and Double Groups*, Oxford Science Publ., Clarendon, Oxford, 1986, pp. 201–223.

[13] Nikravesh, P., Wehage, R., and Kwon, O., "Euler Parameters in Computational Kinematics and Dynamics. Part 1," *Journal of Mechanical Design*, Vol. 107, No. 3, 1985, pp. 358–365. doi:10.1115/1.3260722

[14] Udwadia, F. E., and Schutte, A. D., "Alternative Derivation of the Quaternion Equations of Motion for Rigid-Body Rotational Dynamics," *Journal of Applied Mechanics*, Vol. 77, No. 4, 2010, Paper 044505. doi:10.1115/1.4000917

[15] Schaub, H., and Junkins, J. L., *Analytical Mechanics of Space Systems*, AIAA Education Series, 2nd ed., AIAA, Reston, VA, 2009, pp. 79–199. doi:10.2514/4.867231

[16] Holm, D., *Geometric Mechanics Part II: Rotating, Translating, and Rolling*, Imperial College Press, London, 2011, pp. 19–135.

[17] Goldstein, H., Poole, C., and Safko, J., *Classical Mechanics*, 3rd ed., Addison Wesley, San Francisco, 2001, pp. 34–64, 334–362.

[18] Lanczos, C., *Variational Principles of Mechanics*, 4th ed., Dover, New York, 1986, pp. 35–68.

[19] Morton, H. S., Jr., "Hamiltonian and Lagrangian Formulations of Rigid-Body Rotational Dynamics Based on the Euler Parameters," *Journal of Astronautical Sciences*, Vol. 41, No. 4, 1993, pp. 569–591.

[20] Ascher, U., and Greif, C., *First Course on Numerical Methods*, Computational Science and Engineering, Society for Industrial and Applied Mathematics, Philadelphia, 2011, pp. 251–261.

[21] Hughes, P., *Spacecraft Attitude Dynamics*, Dover Books on Aeronautical Engineering, Dover, New York, 2004, pp. 156–161.

[22] Marsden, J., and Ratiu, T., "Introduction to Mechanics and Symmetry," *Texts in Applied Mathematics*, Springer–Verlag, New York, 1994, pp. 186–191.

[23] Kane, T., and Barba, P., "Effects of Energy Dissipation on a Spinning Satellite," *AIAA Journal*, Vol. 4, No. 8, 1966, pp. 1454–1455. doi:10.2514/3.3703

[24] Shampine, L. F., and Reichelt, M. W., "MATLAB ODE Suite," *SIAM Journal on Scientific Computing*, Vol. 18, No. 1, 1997, pp. 1–22. doi:10.1137/S1064827594276424

[25] Lefferts, E. J., Markley, F. L., and Shuster, M. D., "Kalman Filtering for Spacecraft Attitude Estimation," *Journal of Guidance, Control, and Dynamics*, Vol. 5, No. 5, 1982, pp. 417–429. doi:10.2514/3.56190

[26] Markley, F. L., "Attitude Error Representations for Kalman Filtering," *Journal of Guidance, Control, and Dynamics*, Vol. 26, No. 2, 2003, pp. 311–317. doi:10.2514/2.5048

[27] Black, H. D., "Passive System for Determining the Attitude of a Satellite," *AIAA Journal*, Vol. 2, No. 7, 1964, pp. 1350–1351. doi:10.2514/3.2555